Supporting Information

Supporting Figures

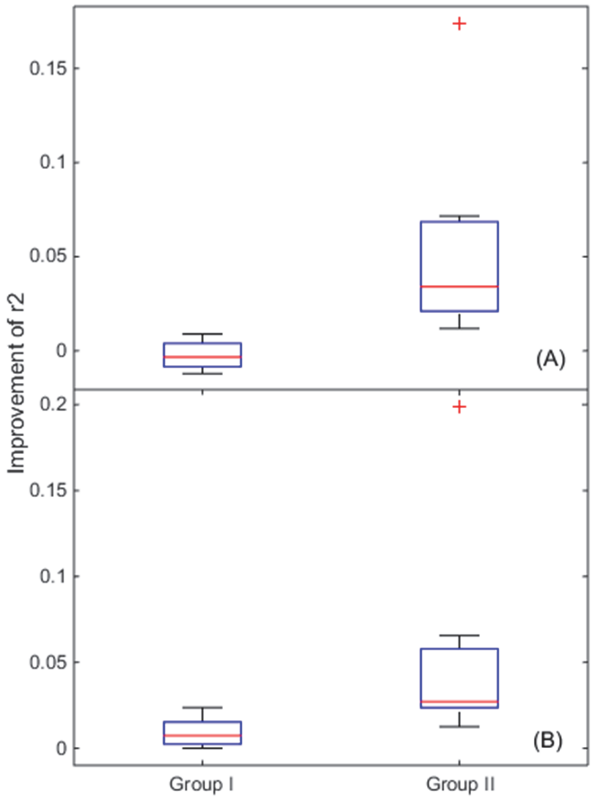

Fig. S1. Influence of the number of ligand samples on the model performance. (A) The improvement in r^2 of the model based on the top-300 features selected from 1,024 bits against the baseline model. (B) The improvement in r^2 of the optimal model (highlighted in boldface in Table 1) against the model based on the top-300 features selected from 1024 bits. Group I: GPCR datasets with more than 600 ligands, i.e., P08908, Q9Y5N1, P28335, P35372, Q99705, P0DMS8, Q16602, P51677, P48039; Group II: GPCR datasets with fewer than 600 ligands, i.e., Q9H228, Q8TDU6, Q8TDS4, Q9HC97, P41180, Q14833, Q99835.

Supporting Tables

Table S1. Description of datasets used in this study

UniProt ID	**Gene Name**	**Protein Name**	**Class**	**Subfamily**	**# of Ligands**	**# of Controls**	**Clinical Significance**
P08908	HTR1A	5-hydroxytryptamine receptor 1A	A	Aminergic receptors	4322	850	Blood pressure, heart rate, antidepressant, anxiolytic, schizophrenia and Parkinson (H Ito, 1999)
Q9Y5N1	HRH3	Histamine H3 receptor	A	Aminergic receptors	3644	700	Cognitive disorders (Esbenshade, et al., 2008)
P28335	HTR2C	5-hydroxytryptamine receptor 2C	A	Aminergic receptors	3286	650	mood, anxiety, feeding, and reproductive behavior(Heisler, et al., 2007)
P35372	OPRM1	Mu-type opioid receptor	A	Peptide receptors	4591	900	Morphine-induced analgesia and itching (Liu, et al., 2011)
Q99705	MCHR1	Melanin-concentrating hormone receptors 1	A	Peptide receptors	3663	700	Appetite, anxiety and depression (Rivera, et al., 2008)
P0DMS8	ADORA3	Adenosine receptor A3	A	Nucleotide receptors	3664	700	Bronchial asthma(Jacobson, et al., 2008)and rheumatoid arthritis(Silverman, et al., 2008)
Q9H228	S1PR5	Sphingosine 1-phosphate receptor 5	A	Lipid receptors	320	60	Huntington's disease(Buttari, 2018)
P51677	CCR3	C-C chemokine receptor type 3	A	Protein receptors	1147	200	Binds and responds to a variety of chemokines (H, et al., 1996)
P48039	MTNR1A	Melatonin receptor type 1A	A	Melatonin receptors	946	190	Circadian rhythm(Slaugenhaupt, et al., 1995)
Q8TDU6	GPBAR1	G-protein coupled bile acid receptor 1	A	Steroid receptors	464	90	Suppression of macrophage functions and regulation of energy homeostasis by bile acids(Wang, et al., 2011)
Q8TDS4	HCAR2	Hydroxycarboxylic acid receptor 2	A	Alicarboxylic acid receptors	500	100	Dyslipidemia(Hu, et al., 2015)
Q9HC97	GPR35	G-protein coupled receptor 35	A	Orphan receptors	330	60	Brachydactyly mental retardation syndrome(Shrimpton, et al., 2004)
Q16602	CALCRL	Calcitonin gene-related peptide type 1 receptor	B	Peptide receptors	691	140	migraine(Edvinsson, 2008)
P41180	CASR	Extracellular calcium-sensing receptor	C	Ion receptors	423	80	Alzheimer's disease, asthma(Kim, et al., 2014)
Q14833	GRM4	Metabotropic glutamate receptor 4	C	Amino acid receptors	548	110	Hallucinogenesis
Q99835	SMO	Smoothened homolog	F	Protein receptors	591	120	Developmental disorders

Table S2. Influence of regression models on the SED performance.

Group[a]	GPCRs	EC[b]	RF	GBDT	SVR	DNN
I	P08908	r^2 (↑)	0.9180	0.9013	0.9027	**0.9314**
		RMSE(↓)	1.0450	1.1556	**0.9015**	0.9879
	Q9Y5N1	r^2 (↑)	0.9380	0.9167	0.9250	**0.9598**
		RMSE(↓)	**0.9470**	1.0886	1.0421	0.9486
	P28335	r^2 (↑)	0.8911	0.8781	0.8895	**0.9095**
		RMSE(↓)	1.1482	1.2048	1.1503	**1.1184**
	P35372	r^2 (↑)	0.8908	0.8697	0.8642	**0.8954**
		RMSE(↓)	1.1660	1.2555	1.2807	**1.1547**
	Q99705	r^2 (↑)	0.9214	0.9142	0.9115	**0.9436**
		RMSE(↓)	0.9959	1.0137	1.0424	**0.8928**
	P0DMS8	r^2 (↑)	0.8880	0.8649	0.8616	**0.8938**
		RMSE(↓)	**1.1650**	1.2719	1.2857	1.1907
	Q16602	r^2 (↑)	0.9489	0.8722	0.7980	**0.9533**
		RMSE(↓)	**0.8795**	1.3374	1.7244	1.4746
	P51677	r^2 (↑)	0.9175	0.8904	0.8860	**0.9405**
		RMSE(↓)	**1.0223**	1.1356	1.1887	1.0280
	P48039	r^2 (↑)	0.9027	0.8571	0.8922	**0.9147**
		RMSE(↓)	**1.2811**	1.4368	1.3275	1.3635
II	Q9H228	r^2 (↑)	0.8725	0.8889	0.8826	**0.9100**
		RMSE(↓)	1.4275	1.2885	**1.2426**	1.3231
	Q8TDU6	r^2 (↑)	0.9275	0.8961	0.8921	**0.9329**
		RMSE(↓)	**0.9789**	1.0694	1.1623	1.0253
	Q8TDS4	r^2 (↑)	0.8912	0.9098	0.9006	**0.9378**
		RMSE(↓)	1.0791	**0.8734**	0.9731	0.9567
	Q9HC97	r^2 (↑)	0.7272	0.5998	0.8371	**0.8508**
		RMSE(↓)	1.7346	1.7818	1.4090	**1.3631**
	P41180	r^2 (↑)	0.7384	0.6673	0.7374	**0.8435**
		RMSE(↓)	1.9836	2.0982	1.8910	**1.5410**
	Q14833	r^2 (↑)	0.7559	0.6268	0.7719	**0.7947**
		RMSE(↓)	1.5008	1.8198	**1.4169**	1.4635
	Q99835	r^2 (↑)	0.8627	0.7840	0.8235	**0.9028**
		RMSE(↓)	1.2819	1.5412	1.3882	**1.1239**

RF: Random Forest, GBDT: Gradient Boosting Decision Tree, SVR: Support Vector Regression, DNN: Deep Neural Network. [a]Group I: original number of ligands ＞600; II: original number of ligands ≤ 600. [b]Evaluation Criterion: ↑ (↓) indicates that larger (smaller) values are better; the best results for each evaluation criterion are highlighted in boldface. The input of each regression model was the top-300 features selected from the optimal bits of the ECFPs. For each GPCR dataset, the optimal bit is the ECFP length corresponding to the optimal result (highlighted in boldface in Table 1).

Table S3. Comparison of SED with the WDL-RF method

Group[a]	GPCRs	EC[b]	WDL-RF	SED[c]
I	P08908	r^2 (↑)	0.7062	0.9314*
		RMSE(↓)	1.5038	0.9879*
	Q9Y5N1	r^2 (↑)	0.8242	0.9598*
		RMSE(↓)	1.6293	0.9486*
	P28335	r^2 (↑)	0.5764	0.9095*
		RMSE(↓)	2.2714	1.1184*
	P35372	r^2 (↑)	0.7428	0.8954*
		RMSE(↓)	1.5127	1.1547*
	Q99705	r^2 (↑)	0.8236	0.9436*
		RMSE(↓)	1.3342	0.8928*
	P0DMS8	r^2 (↑)	0.7580	0.8938*
		RMSE(↓)	1.6753	1.1907*
	Q16602	r^2 (↑)	0.7482	0.9533*
		RMSE(↓)	0.8153	1.4746*
	P51677	r^2 (↑)	0.8491	0.9405*
		RMSE(↓)	1.3391	1.0280*
	P48039	r^2 (↑)	0.7874	0.9147*
		RMSE(↓)	1.8357	1.3635*
II	Q9H228	r^2 (↑)	0.5839	0.9100*
		RMSE(↓)	0.6165	1.3231*
	Q8TDU6	r^2 (↑)	0.7303	0.9329*
		RMSE(↓)	1.6806	1.0253*
	Q8TDS4	r^2 (↑)	0.4556	0.9378*
		RMSE(↓)	0.7637	0.9567*
	Q9HC97	r^2 (↑)	0.4797	0.8508*
		RMSE(↓)	0.7764	1.3631*
	P41180	r^2 (↑)	0.6619	0.8435*
		RMSE(↓)	2.0476	1.5410*
	Q14833	r^2 (↑)	0.4169	0.7947*
		RMSE(↓)	0.8373	1.4635*
	Q99835	r^2 (↑)	0.4834	0.9028*
		RMSE(↓)	2.1368	1.1239*

[a]Group I: original number of ligands ＞600; II: original number of ligands ≤ 600. [b]Evaluation Criterion: ↑ (↓) indicates that larger (smaller) values are better. [c]SED: For each GPCR dataset, the optimal result was selected for comparison (highlighted in boldface in Table 1). * indicates that the performance of the SED method is significantly better than that of the WDL-RF methods (Wu, et al., 2018) based on Wilcoxon signed-rank test.

Table S4. Top 51 to 300 Substructures Identified by SED Accompanying with the Associated Pearson Correlation Coefficients.

Top 51-60 (Pearson correlation)	Top 61-70 (Pearson correlation)	Top 71-80 (Pearson correlation)	Top 81-90 (Pearson correlation)	Top 91-100 (Pearson correlation)
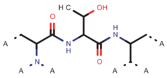 -0.162	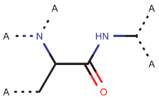 -0.162	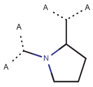 -0.162	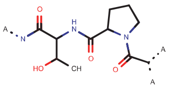 -0.162	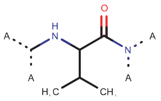 -0.162
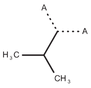 -0.162	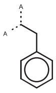 -0.162	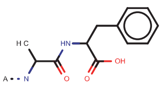 -0.162	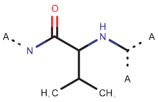 -0.162	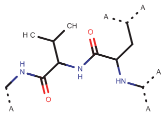 -0.162
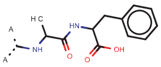 -0.162	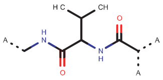 -0.162	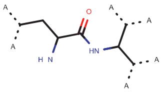 -0.162	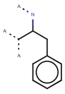 -0.162	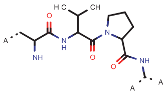 -0.162
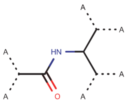 -0.162	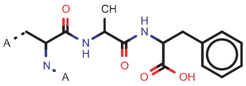 -0.162	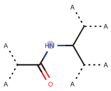 -0.162	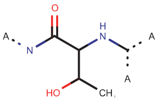 -0.162	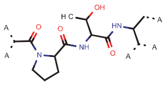 -0.162
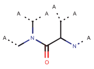 -0.162	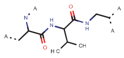 -0.162	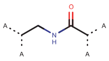 -0.162	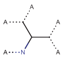 -0.162	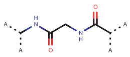 -0.162
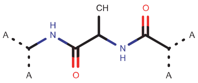 -0.162	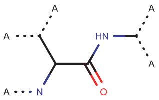 -0.162	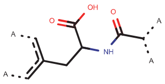 -0.162	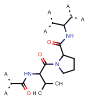 -0.162	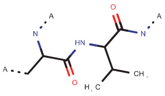 -0.162
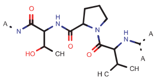 -0.162	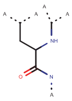 -0.162	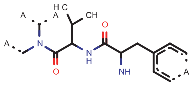 -0.162	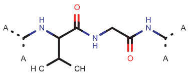 -0.162	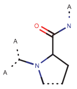 -0.162
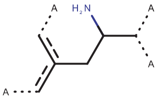 -0.162	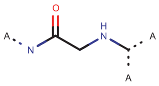 -0.162	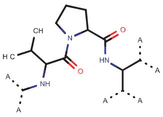 -0.162	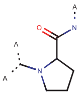 -0.162	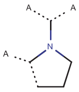 -0.162
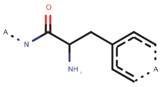 -0.162	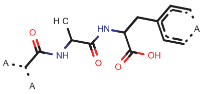 -0.162	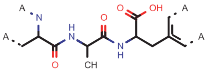 -0.162	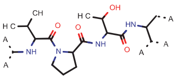 -0.162	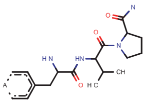 -0.162
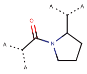 -0.162	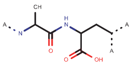 -0.162	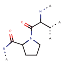 -0.162	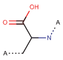 -0.162	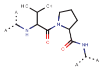 -0.162

(Table S4 Continued)

Top 101-110 (Pearson correlation)	Top 111-120 (Pearson correlation)	Top 121-130 (Pearson correlation)	Top 131-140 (Pearson correlation)	Top 141-150 (Pearson correlation)
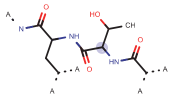 -0.162	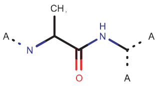 -0.162	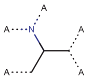 -0.162	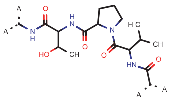 -0.162	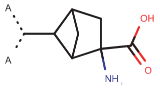 -0.115
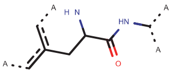 -0.162	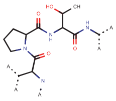 -0.162	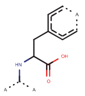 -0.162	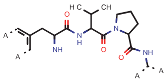 -0.162	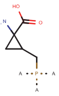 -0.115
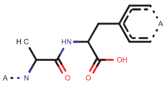 -0.162	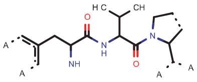 -0.162	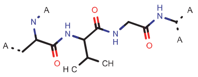 -0.162	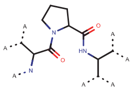 -0.162	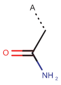 -0.199
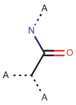 -0.162	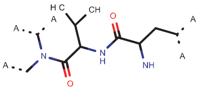 -0.162	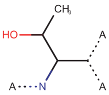 -0.162	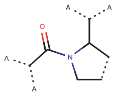 -0.162	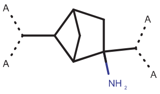 -0.115
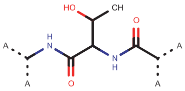 -0.162	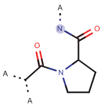 -0.162	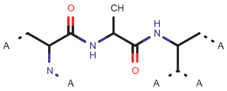 -0.162	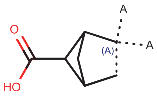 -0.115	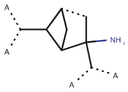 -0.115
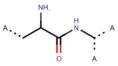 -0.162	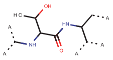 -0.162	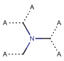 -0.162	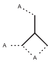 -0.115	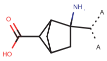 -0.115
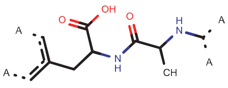 -0.162	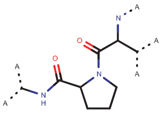 -0.162	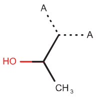 -0.162	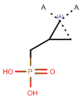 -0.115	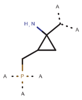 -0.115
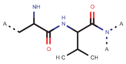 -0.162	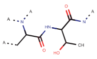 -0.162	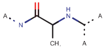 -0.162	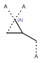 -0.115	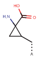 -0.115
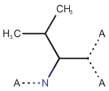 -0.162	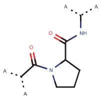 -0.162	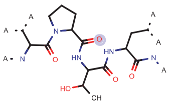 -0.162	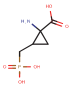 -0.115	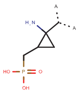 -0.115
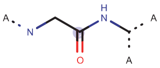 -0.162	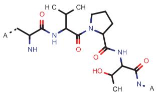 -0.162	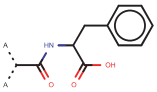 -0.162	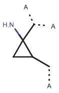 -0.115	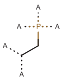 -0.115

(Table S4 Continued)

Top 151-160 (Pearson correlation)	Top 161-170 (Pearson correlation)	Top 171-180 (Pearson correlation)	Top 181-190 (Pearson correlation)	Top 191-200 (Pearson correlation)
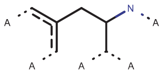 -0.23	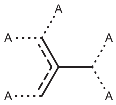 -0.214	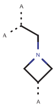 0.28	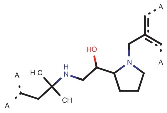 -0.162	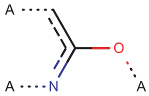 -0.199
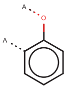 -0.199	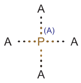 0.288	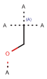 0.191	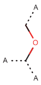 0.223	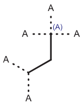 -0.347
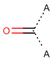 -0.484	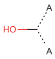 -0.134	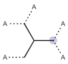 -0.199	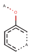 -0.159	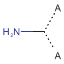 -0.23
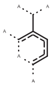 -0.162	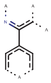 -0.162	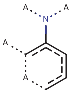 -0.326	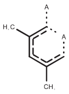 -0.199	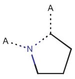 -0.122
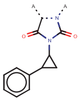 -0.199	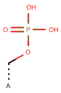 0.237	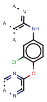 -0.162	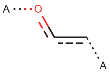 -0.162	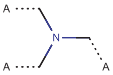 0.291
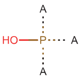 0.288	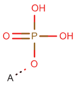 0.242	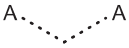 0.04	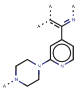 -0.199	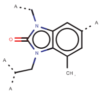 -0.199
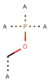 0.255	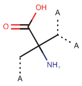 -0.133	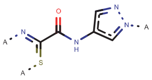 -0.199	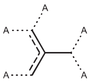 -0.267	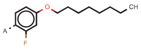 0.033
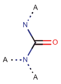 -0.367	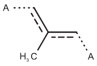 -0.196	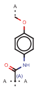 0.063	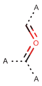 -0.162	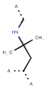 -0.23
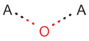 0.276	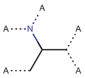 -0.199	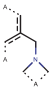 0.299	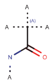 -0.347	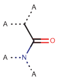 -0.306
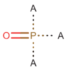 0.276	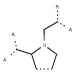 -0.199	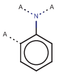 -0.257	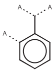 -0.258	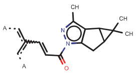 0.022

(Table S4 continued)

Top 201-210 (Pearson correlation)	Top 211-220 (Pearson correlation)	Top 221-230 (Pearson correlation)	Top 231-240 (Pearson correlation)	Top 241-250 (Pearson correlation)
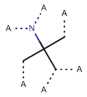 -0.258	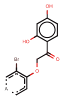 -0.115	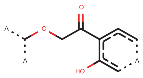 -0.115	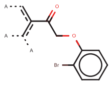 -0.115	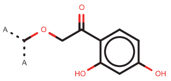 -0.115
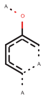 0.211	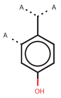 -0.115	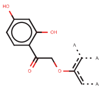 -0.115	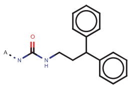 -0.162	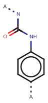 -0.162
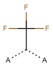 0.17	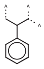 -0.162	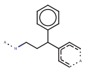 -0.162	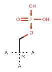 0.162	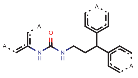 -0.162
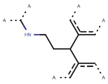 -0.162	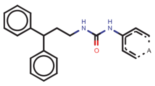 -0.162	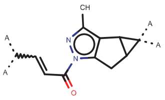 0.036	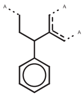 -0.162	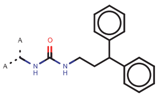 -0.162
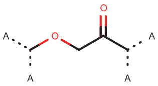 -0.115	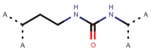 -0.162	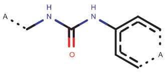 -0.162	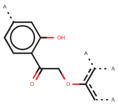 -0.115	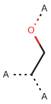 -0.115
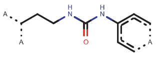 -0.162	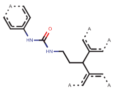 -0.162	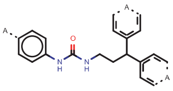 -0.162	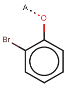 -0.115	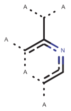 -0.199
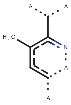 -0.199	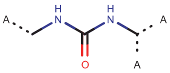 -0.162	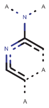 -0.258	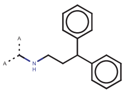 -0.162	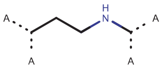 -0.162
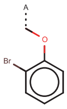 -0.115	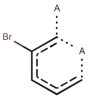 -0.115	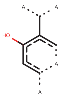 -0.115	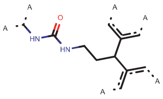 -0.162	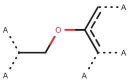 -0.115
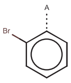 -0.115	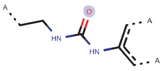 -0.162	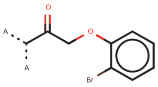 -0.115	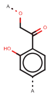 -0.115	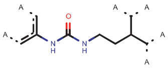 -0.162
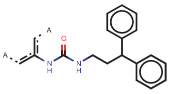 -0.162	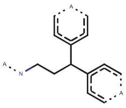 -0.162	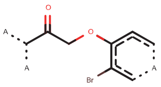 -0.115	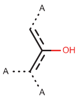 -0.115	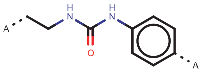 -0.162

(Table S4 continued)

Top 251-260 (Pearson correlation)	Top 261-270 (Pearson correlation)	Top 271-280 (Pearson correlation)	Top 281-290 (Pearson correlation)	Top 291-300 (Pearson correlation)
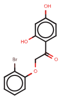 -0.115	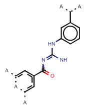 -0.162	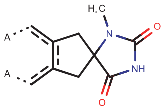 -0.23	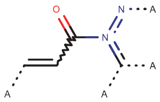 0.021	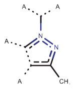 0.021
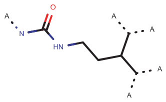 -0.162	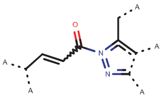 0.021	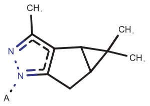 0.021	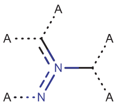 0.021	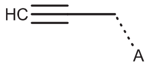 -0.115
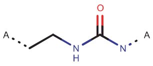 -0.162	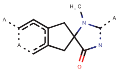 -0.23	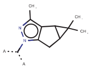 0.021	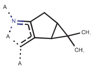 0.021	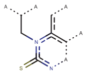 -0.115
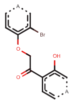 -0.115	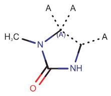 -0.23	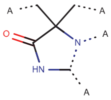 -0.23	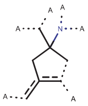 -0.23	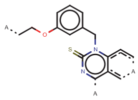 -0.115
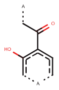 -0.115	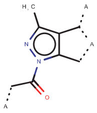 0.021	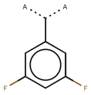 -0.199	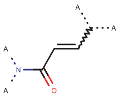 0.021	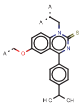 -0.115
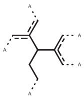 -0.162	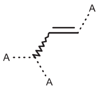 0.021	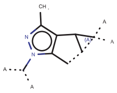 0.021	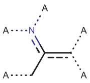 0.021	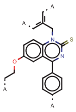 -0.115
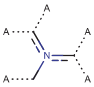 -0.23	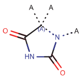 -0.23	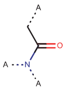 0.021	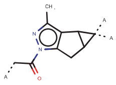 0.021	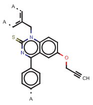 -0.115
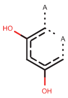 -0.115	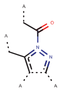 0.021	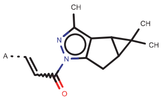 0.021	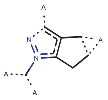 0.021	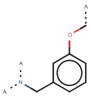 -0.115
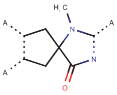 -0.23	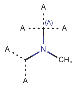 -0.23	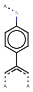 -0.162	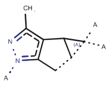 0.021	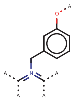 -0.115
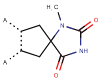 -0.23	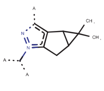 0.021	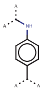 -0.162	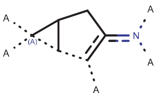 0.021	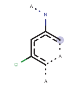 -0.162

Supporting Texts

Text S1. Code usage of SED

We have developed a demonstration program for the sparse screening of ECFPs and ligand-based virtual screening; the source codes and datasets are available through https://zhanglab.ccmb.med.umich.edu/SED/. The code for SED was developed in Matlab2014, Python 2.7. This provides a general framework for the screening for Lasso of ECFPs and ligand-based virtual screening, which allows users to develop their own key substructure recognition and virtual screening tools for the drug targets of their choice on the basis of our code. The program GenerateMD for the generation of ECFPs is authorized by the ChemAxon Ltd. with the free license for academic research. Due to the copyright issues, we provided the open-source cheminformatics software RDKit for generating the Morgan fingerprints which are a suitable alternative of ECFPs here.

Input: Compounds in the format of canonical SMILES and their bioactivity values.

Output: Model performance (*RMSE*, r^2).

The procedure of the pipeline is as follows: Input compounds in the format of canonical SMILES and their bioactivity values → Generate fingerprints by RDKit → Obtain top features selected by Lasso screening of fingerprints → Rebuild the ligand dataset using the selected top features → Construct DNN regression models → Obtain the model performance. The details of implementing the SED package can see the README.txt file through https://zhanglab.ccmb.med.umich.edu/SED/README.txt.

References

Alba D.P., *et al.* (2018) Stimulation of S1PR5 with A-971432, a selective agonist, preserves blood–brain barrier integrity and exerts therapeutic effect in an animal model of Huntington's disease, *Human Molecular Genetics*, **27**:2490-2501.

Edvinsson, L. (2008) CGRP-receptor antagonism in migraine treatment, *Lancet*, **372**, 2089-2090.

Esbenshade, T.A., *et al.* (2008) The histamine H3 receptor: an attractive target for the treatment of cognitive disorders, *British Journal of Pharmacology*, **154**, 1166-1181.

H, C., *et al.* (1996) The beta-chemokine receptors CCR3 and CCR5 facilitate infection by primary HIV-1 isolates, *Cell*, **85**, 1135-1148.

H Ito, C.H., L Farde (1999) Localization of 5-HT1A receptors in the living human brain using [carbonyl-11C]WAY-100635: PET with anatomic standardization technique, *Journal of Nuclear Medicine*, **40**, 102-109.

Heisler, L.K., *et al.* (2007) Serotonin 5-HT(2C) receptors regulate anxiety-like behavior, *Genes Brain & Behavior*, **6**, 491-496.

Hu, M., *et al.* (2015) Pharmacogenetics of cutaneous flushing response to niacin/laropiprant combination in Hong Kong Chinese patients with dyslipidemia, *Pharmacogenomics*, **16**, 1387-1397.

Jacobson, K.A., *et al.* (2008) Flexible modulation of agonist efficacy at the human A 3 adenosine receptor by the imidazoquinoline allosteric enhancer LUF6000, *Bmc Pharmacology*, **8**, 20.

Kim, J.Y., *et al.* (2014) Calcium-sensing receptor (CaSR) as a novel target for ischemic neuroprotection, *Annals of Clinical & Translational Neurology*, **1**, 851-866.

Liu, X.Y., *et al.* (2011) Unidirectional cross-activation of GRPR by MOR1D uncouples itch and analgesia induced by opioids, *Cell*, **147**, 447-458.

Rivera, G., *et al.* (2008) Melanin-concentrating hormone receptor 1 antagonists: a new perspective for the pharmacologic treatment of obesity, *Current Medicinal Chemistry*, **15**, 1025-1043.

Shrimpton, A.E., *et al.* (2004) Molecular delineation of deletions on 2q37.3 in three cases with an Albright hereditary osteodystrophy-like phenotype, *Clinical Genetics*, **66**, 537-544.

Silverman, M.H., *et al.* (2008) Clinical evidence for utilization of the A3 adenosine receptor as a target to treat rheumatoid arthritis: data from a phase II clinical trial, *Journal of Rheumatology*, **35**, 41-48.

Slaugenhaupt, S.A., *et al.* (1995) Mapping of the gene for the Mel 1a-melatonin receptor to human chromosome 4 (MTNR1A) and mouse chromosome 8 (Mtnr1a), *Genomics*, **27**, 355-357.

Wang, Y.D., *et al.* (2011) The G-Protein-coupled bile acid receptor, Gpbar1 (TGR5), negatively regulates hepatic inflammatory response through antagonizing nuclear factor kappa light-chain enhancer of activated B cells (NF-κB) in mice, *Hepatology*, **54**, 1421-1432.

Wu, J., *et al.* (2018) WDL-RF: Predicting Bioactivities of Ligand Molecules Acting with G Protein-coupled Receptors by Combining Weighted Deep Learning and Random Forest, *Bioinformatics*,**34**, 2271-2282.